



Ball's-Based Adaptive Channel Estimation Scheme Using RLS Family-Types Algorithms

Ali Al-Shuwaili¹, Mustafa Dh. Hassib² and Thamer M. Jamel²

¹Media Technology and Communications Engineering Department, University of Information Technology and Communications, Baghdad, Iraq

²Department of the Communications Engineering, University of Technology, Baghdad, Iraq

Received 23 Jul. 2021, Revised 27 Jul. 2022, Accepted 31 Jul. 2022, Published 6 Aug. 2022

Abstract: the recovery of the transmitted signals, propagated through wireless communication channels, is a complicated process due to the distortion and interference impairments in such random channels. However, the channel effect can be compensated by using channel estimation techniques performed at the receiver. Since most of channel estimators are operated in the frequency domain, i.e., inverse modeling, the Ball's adaptive channel estimation scheme, which was invented by Michael J. Ball, was not considered in the literature as an attractive approach due to its time-based and direct modeling features. However, such features are favorable for time-varying channels. To the best of author's knowledge, the performance of the Ball's scheme for channel estimation has not been investigated in the context of OFDM system with fading channels. Therefore, in this paper, we propose to incorporate Ball's method for channel estimation in OFDM receivers and we also investigate the performance of this scheme using variations of the Recursive Least Squares (RLS)-type algorithms, namely QR Decomposition RLS (QRD-RLS), the Householder RLS (HH-RLS) and the Sliding Window Householder RLS (SWHH-RLS). Our numerical results indicate that QRD-RLS and HH-RLS outperform traditional RLS in terms of bit error rate.

Keywords: Ball's scheme, adaptive channel estimation, recursive least square, QR-decomposition, householder, sliding window RLS, OFDM.

1. INTRODUCTION

Wireless mobile radio channels are often multipath channels. In such channels, two or more versions of the transmitted signal, i.e., the direct signals, or Line-of-Sight (LOS) signals, and signals reflected or scattered by objects in the medium, i.e., Non-Line-of-Sight (NLOS) signals reach the receiving antenna. The aggregated multipath components at the receiver yield a signal that is highly distorted in amplitude, phase and frequency resulting in an effect called multipath fading [1], [2].

Multipath propagation causes smearing of the symbols transmitted through the channel. This smearing will lengthen the interval of the symbols resulting in what is known as Inter-Symbol Interference (ISI) which degrade system performance highly [1], [2]. To improve the Bit Error Rate (BER) performance, or increase the number of correctly-decoded symbols, the channel distortion need to

be identified using channel estimation and then compensated using equalization techniques, at the receiver [3], [4]. Since the multipath fading channel is random and time-varying, channel estimator and equalizer must be adaptive, i.e., able to track the varying channel. The adaptive estimator or equalizer is basically an adaptive filter with coefficients that are automatically adjusted with the aid of the adaptive algorithms [4], [5], [6].

Orthogonal Frequency Division Multiplexing (OFDM) is a modulation technique suitable for high-speed multi-carrier data transmission [7]. In a typical OFDM system, a Cyclic Prefix (CP) is utilized to alleviate the effect of ISI by allowing more spacing between subcarriers. Because CP bears no useful information, the use of CP reduces bandwidth efficiency especially under severe channel conditions that requires the duration of CP to be long. Thus, channel estimation is one key component in OFDM systems

by allowing the receiver side to obtain information about the channel in terms of Channel State Information (CSI) [1], [2]. Typically, the CSI is not known at the receiver and also changing continuously due to the changing environment. Therefore, adaptive channel estimators are deployed at the receiver side to track the time-varying channel via the utilization of adaptive algorithms. In more details, the CSI is estimated using pilots symbols in the training phase. Afterward, data symbols can be transmitted reliably during transmission phase benefiting from the CSI obtained in the first phase [8], [9].

Traditional channel estimators work by estimating the Channel Frequency Response (CFR) [10]. First, pilot-based estimation of CFRs for some training symbols is performed [11], [12]. Then, CFRs of data symbols are estimated using the adaptive algorithms and techniques [13], [14], [15], [16]. For instance the work [15], [16] considers pilot-assisted estimator which operated with the maximum likelihood (ML) and the Bayesian minimum mean square error (MMSE) techniques. Alternatively, with advent of Machine Learning (ML) algorithms and its applications in signal processing and communications, several work have shown the effectiveness of ML-based approaches, like deep learning [17], [18], [19], [20] and reinforcement learning [21], in performing adaptive channel estimation.

Along with the increase importance of Multiple-Input Multiple-Output (MIMO) in achieving higher capacity for fading channels and also enhancing system throughput, MIMO-OFDM receivers become standard in many wireless applications [22], [23]. However, the Single-Input Single-Output (SISO) channel estimation techniques discussed above can not be applied directly to MIMO-OFDM systems. As a results, several work address this problem. The work in [24] relies on Discrete Fourier Transform (DFT) to derive the set of training signals which minimize the estimator MSE. A blind and semi-blind MIMO channel estimators are proposed in [25] and [26], [27], respectively.

The literature summarized above consider mainly a frequency-domain channel estimation for OFDM system. A relevant, but less interesting, line of work have dealt with the time-domain based channel estimation as in [28] where a LMMS estimator is proposed with pilot-data multiplexing and compared to the scheme in [29] which relies on pilots tones. The work in [30] shows that Kalman filtering-based channel estimation is suitable to track and estimate fading channels. A comparison between time-domain and frequency-domain channel estimation for OFDM system are discussed in [31], [32]. Even with this line of work, the channel estimation scheme for multipath communications proposed in [4], which was invented by Michael J. Ball,

did not receive much attention in the literature. This is because most of channel estimators are performed in the frequency domain, i.e., inverse modeling (see Fig. 1-(a)). On the contrary, the Ball's channel estimation scheme tries to equalize the communications channel directly (see Fig. 1-(b)) as the inverse of the channel frequency response is not required. This time-based and direct modeling features of the Ball's scheme are favorable for modeling, i.e., estimating multipath and rapidly time-varying channels like intelligent reflecting surface (IRS)-enabled radio links [33], [34]. Unlike previous work, in this paper, we proposes to leverage Ball's-based channel estimation scheme in OFDM systems using different types of RLS algorithm. The standard RLS algorithm have been applied in several adaptive filtering applications [35], [4], [8], [36]. Most of these applications show a performance gain under different channel conditions, but they incur extra complexity in computations and raise some stability issues. Therefore, we will investigate the performance of the proposed scheme under different types of the RLS algorithm. In details, the major contributions of this work are:

- Design an OFDM system receiver by utilizing the Ball's method for channel estimation.
- Investigate the performance of the proposed approach using, in addition to conventional RLS, the QR Decomposition RLS (QRD-RLS), the Householder RLS (HH-RLS) and the Sliding Window Householder RLS (SWHH-RLS). It is the first time here that this set of RLS algorithms is used in an OFDM receivers as well as in investigating the performance of the proposed scheme.
- Conduct numerical experiments and select the suitable set of algorithms that best fit the proposed scheme by balancing both the convergence speed and the complexity of computations.

The rest of the paper is organized as follows. The family of RLS-type algorithms are explained in Section 3 after presenting the proposed scheme in Section 2. The simulation results are shown in Section 4 Finally, conclusions are outlined in Section 5.

Notations: We use lowercase bold letters to denote vectors while matrices are denoted by uppercase bold letters. For a matrix \mathbf{A} , the notations \mathbf{A}^{-1} , \mathbf{A}^T and \mathbf{A}^H denote its inverse, transpose, and Hermitian transpose respectively. Scalars are denoted by lowercase letters.

2. BALL'S BASED ADAPTIVE CHANNEL ESTIMATION

Apart from conventional channel estimation schemes, the Ball's scheme brings two unique features: channel

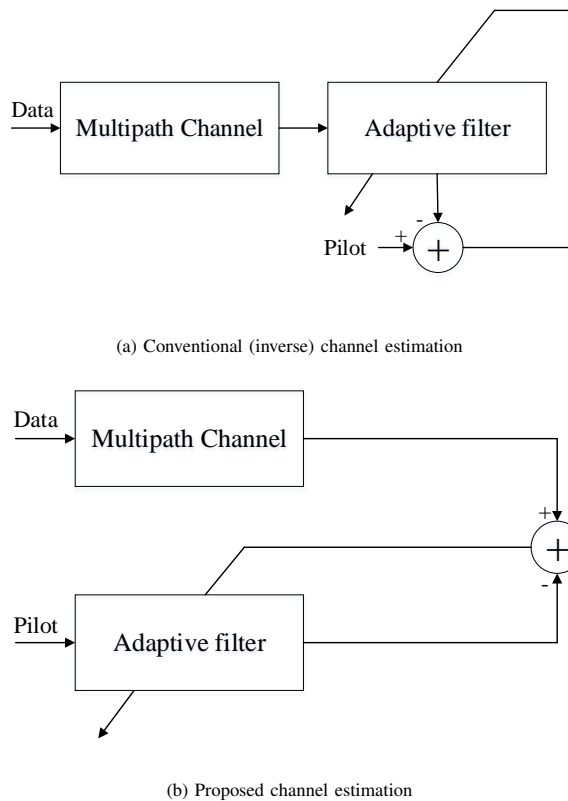


Figure 1. Channel estimation schemes: (a) Conventional inverse modeling scheme; (b) Proposed Ball-based scheme.

impulse response is estimated in time domain, and also the ability to perform direct channel equalization since channel frequency response inversion is not required (see Fig. 1). The actual operation of this adaptive scheme is described next.

As illustrated in Fig. 2, the transmitted signal is produced as Pseudo Random (PN) sequence of data. At the receiver, the channel estimator, or adaptive filter, will tune its coefficients based on the Least-Square (LS) of the error, or the difference between output of the filter and the output of the channel. As a reference, the filter uses synchronized and local version of the PN sequence. The optimal weight of the adaptive filter in Fig. 2 is the well-known Wiener solution formulated as

$$\mathbf{h}(n) = \mathbf{F}^{-1}(n)\mathbf{c}(n), \quad (1)$$

where \mathbf{F} is the correlation matrix of input data \mathbf{U} as given in

$$\mathbf{F}(n) = \sum_{i=0}^n \tau^{n-i} \mathbf{u}(i)\mathbf{u}(i)^H = \mathbf{U}^H(n)\mathbf{U}(n), \quad (2)$$

while \mathbf{c} is the vector denoting the cross correlation of

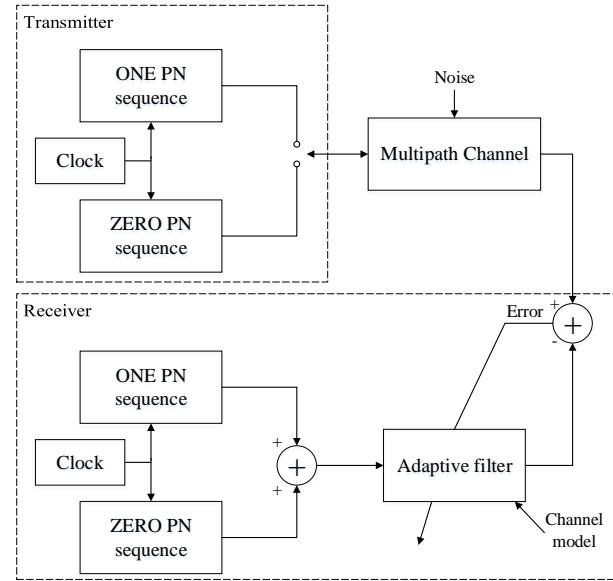


Figure 2. Block diagram of the adaptive Ball's-based scheme for channel estimation during actual data transmission [4].

desired response \mathbf{g} and input data which is formulated as [4], [35]

$$\mathbf{c}(n) = \sum_{i=0}^n \tau^{n-i} \mathbf{g}(i)\mathbf{u}(i) = \mathbf{U}^H(n)\mathbf{g}(n), \quad (3)$$

with τ being the forgetting parameter. The optimal Wiener filter in (1) is obtained as the solution that minimizes the Mean Square Error (MSE) objective function written as

$$\varepsilon(n) = \mathbb{E} [\mathbf{e}^2(n)] = \mathbb{E} [|\mathbf{g}(n) - \mathbf{h}^T(n)\mathbf{u}(n)|^2]. \quad (4)$$

In every time epoch, denoted as n in (1)-(4), the components in the weight vector $\mathbf{h}(n)$ are updated according to the adopted algorithm. The set of algorithms considered in this paper are presented in the next section.

3. ADAPTIVE RLS-TYPE ALGORITHMS

In this section, we will give a detailed description for each algorithm considered in this work, namely RLS, QRD-RLS, HH-RLS and SWHH-RLS.

A. Recursive-Least-Squares (RLS) algorithm

Despite the fact that RLS algorithm has rapid convergence feature, it is still requires high computational complexity and can experience some stability issues. To proceed, we rewrite correlation matrix \mathbf{F} and the vector of cross correlation \mathbf{c} defined in (2) and (3), respectively, as [4], [35]

$$\mathbf{F}(n) = \mathbf{u}(n)\mathbf{u}^H(n) + \tau\mathbf{F}(n-1) \quad (5)$$

and

$$\mathbf{c}(n) = \mathbf{u}(n)\mathbf{g}(n) + \tau\mathbf{c}(n-1). \quad (6)$$

By plugging (5) and (6) in (1), we obtain the following weight update formula

$$\mathbf{h}(n) = \mathbf{h}(n-1) + \mathbf{e}(n)\mathbf{F}^{-1}(n)\mathbf{u}(n), \quad (7)$$

where the error vector $\mathbf{e}(n)$ and \mathbf{F}^{-1} are calculated as shown in Algorithm 1. This table summarizes the steps required for the RLS algorithm with $\mathbf{\Gamma}(n)$ and $\mathbf{\Lambda}(n)$ being an auxiliary vectors, while τ and ϵ are forgetting and gain factors, respectively.

Algorithm 1: RLS algorithm

initialization: $0 \ll \tau < 1$, $\epsilon \approx 1/\sigma_u^2$, $\mathbf{F}^{-1}(0) = \epsilon\mathbf{I}$

for all n do

$$\mathbf{e}(n) = \mathbf{g}(n) - \mathbf{h}^H(n-1)\mathbf{u}(n)$$

$$\mathbf{\Lambda}(n) = \mathbf{F}^{-1}(n-1)\mathbf{u}(n);$$

$$\mathbf{\Gamma}(n) = \frac{\mathbf{\Lambda}(n)}{\tau + \mathbf{u}^H(n)\mathbf{\Lambda}(n)}$$

$$\mathbf{F}^{-1}(n) = \frac{1}{\tau} \left[\mathbf{F}^{-1}(n-1) - \frac{\mathbf{\Gamma}(n)\mathbf{\Lambda}^H(n)}{\tau + \mathbf{u}^H(n)\mathbf{\Lambda}(n)} \right]$$

$$\mathbf{h}(n) = \mathbf{h}(n-1) + \mathbf{e}(n)\mathbf{\Gamma}(n)$$

end

B. QR decomposition (QRD-RLS) algorithm

To avoid the stability problem of RLS procedures mentioned earlier, different approach with enhanced numerical stability is offered by the QRD-RLS algorithm. This implementation relies essentially on QR factorization for the matrix of input data along with back substitution procedures [4], [35]. To proceed, we first note that the matrix $\mathbf{u}(n)$ has dimensions $(n+1) \times (N+1)$ which dictate that the matrix order depends on the number of iterations. Accordingly, the QRD-RLS convert $\mathbf{u}(n)$ into a triangular matrix $\mathbf{T}(n)$ of order $(N+1) \times (N+1)$ via an orthogonal matrix $\mathbf{\Theta}(n)$ of order $(n+1) \times (n+1)$ such that [4], [35]

$$\mathbf{\Theta}(n)\mathbf{u}(n) = \begin{bmatrix} \mathbf{0} \\ \mathbf{T}(n) \end{bmatrix}, \quad (8)$$

where $\mathbf{0}_{(n-N) \times (N+1)}$ denotes an array of zeros with unitary matrix $\mathbf{\Theta}(n)$ represents the triangularization steps. Based on (8), we can rewrite $\mathbf{U}(n)$ as

$$\mathbf{U}(n) = \mathbf{\Theta}_2^H(n)\mathbf{T}(n), \quad (9)$$

where $\mathbf{\Theta}_2^H(n)$ is a unitary matrix partition with size $(n+N) \times (n+1)$. Thus, we rewrite $\mathbf{F}(n)$ as

$$\mathbf{F}(n) = \mathbf{U}^H(n)\mathbf{U}(n) = \mathbf{T}^H(n)\mathbf{T}(n), \quad (10)$$

where $\mathbf{T}(n)$ denotes the Cholesky factor of (10). The rotated error vector $(n+1) \times 1$ is expressed as

$$\mathbf{e}_q(n) = \mathbf{\Theta}(n)\mathbf{e}(n) = \begin{bmatrix} \mathbf{e}_{q1}(n) \\ \mathbf{e}_{q2}(n) \end{bmatrix} = \begin{bmatrix} \mathbf{g}_{q1}(n) \\ \mathbf{g}_{q2}(n) \end{bmatrix} - \begin{bmatrix} \mathbf{0} \\ \mathbf{T}(n) \end{bmatrix} \mathbf{h}(n). \quad (11)$$

The weight vector $\mathbf{h}(n)$ is selected so as the quantity in (11) is optimized, i.e., the weighted-square error function is minimized. It follows that by choosing

$$\mathbf{h}(n) = \mathbf{T}^{-1}(n)\mathbf{g}_{q2}(n), \quad (12)$$

the term $\mathbf{T}^{-1}(n)\mathbf{g}_{q2}(n)$ in (11) will vanish. The updating steps of QRD-RLS algorithm are illustrated in Algorithm 2.

Algorithm 2: QRD-RLS algorithm

for all n do

Computing $\mathbf{\Theta}_\theta(n)$ and updating $\mathbf{T}(n)$:

$$\begin{bmatrix} \mathbf{0}^H \\ \mathbf{T}(n) \end{bmatrix} = \mathbf{\Theta}_\theta(n) \begin{bmatrix} \mathbf{u}^H(n) \\ \sqrt{\tau}\mathbf{T}(n-1) \end{bmatrix}$$

Computing $\gamma(n)$: $\gamma(n) \triangleq \prod_{i=0}^N \cos \theta_i(n)$

Computing $\mathbf{e}_{q1}(n)$ and $\mathbf{g}_{q2}(n)$:

$$\begin{bmatrix} \mathbf{e}_{q1}(n) \\ \mathbf{g}_{q2}(n) \end{bmatrix} = \mathbf{\Theta}_\theta(n) \begin{bmatrix} \mathbf{g}^*(n) \\ \sqrt{\tau}\mathbf{g}_{q2}(n-1) \end{bmatrix}$$

Computing $\epsilon_{q1}(n)$:

$$\epsilon_{q1}(n) \triangleq \mathbf{e}_{q1}(n)\gamma(n)$$

end

C. Householder (HH-RLS) algorithm

Most of QRD-RLS implementations utilize Gram-Schmidt process and Givens rotation method to orthogonalize the data correlation matrix, but none of these approaches is computationally efficient. Instead, the Householder transformation is a rank- n update approach with orthogonal matrix transform. Consequently, HH-RLS requires less computations and provides numerical stability even for sparse data structure. The key property of this algorithm is that, at each iteration, the Cholesky factor of \mathbf{F} is updated. Define the square matrix $\mathbf{Z}(n)$ of order $N+1$ to be factor for the square root of \mathbf{F} , then we can write

$$\mathbf{F}(n) = \mathbf{Z}^H(n)\mathbf{Z}(n). \quad (13)$$

Next, we define

$$\mathbf{b}(n) = \frac{\mathbf{Z}^{-T}(n-1)\mathbf{u}(n)}{\sqrt{\tau}}, \quad (14)$$

where τ denotes the forgetting parameter. We define the orthogonal Householder matrix $\mathbf{a}(n)$ of order $(N+2) \times (N+2)$ [4], [35], to formulate

$$\mathbf{a}(n) \begin{bmatrix} \mathbf{1} \\ \mathbf{b}(n) \end{bmatrix} = \begin{bmatrix} -\zeta(n) \\ \mathbf{0} \end{bmatrix}, \quad (15)$$

with $\zeta(n)$ being a positive scalar. It is left to mention that HH-RLS algorithm computes error and weight vectors according to the formulas

$$\mathbf{e}(n) = \mathbf{g}(n) - \mathbf{h}^H(n-1) \mathbf{u}(n) \quad (16)$$

with

$$\mathbf{h}(n) = \mathbf{h}(n-1) - \frac{\mathbf{e}(n)}{\zeta(n)} \mathbf{v}(n), \quad (17)$$

respectively, with $\mathbf{v}(n)$ being the scaled gain vector. The complete description of HH-RLS is given in the following algorithm.

Algorithm 3: HH-RLS algorithm

initialization: $0 \ll \tau < 1$, $\epsilon \approx 1/\sigma_u^2$, $\mathbf{h}(0) = \mathbf{0}$,

$$\mathbf{Z}^{-1}(0) = \sqrt{\epsilon} \mathbf{I}$$

for all n do

 Computing $\mathbf{b}(n)$ using (14)

$$\text{Finding } \mathbf{a}(n) \text{ and } \zeta(n): \mathbf{a}(n) \begin{bmatrix} \mathbf{1} \\ \mathbf{b}(n) \end{bmatrix} = \begin{bmatrix} -\zeta(n) \\ 0 \end{bmatrix}$$

 Computing $\mathbf{Z}^{-1}(n-1)$:

$$\mathbf{a}(n) \begin{bmatrix} \mathbf{0}^H \\ \tau^{-1/2} \mathbf{Z}^{-H}(n-1) \end{bmatrix} = \begin{bmatrix} \mathbf{v}^H(n) \\ \mathbf{Z}^{-H}(n) \end{bmatrix}$$

 Computing $\mathbf{e}(n)$ using (16) and $\mathbf{h}(n)$ using (17)

end

D. Sliding Window Householder (SWHH-RLS) Algorithm

For efficient computations of HH-RLS, the complexity can be reduced by applying a sliding window (SW) on the input which organized into blocks of size Q . In a mathematical formulation, we write [4], [35]

$$\mathbf{e}(n) = \begin{bmatrix} e_n \\ e_{n-1} \\ \vdots \\ e_{n-L+1} \end{bmatrix} = \mathbf{g}(n) - \mathbf{U}(n) \mathbf{h}(n), \quad (18)$$

where L is the size of the window with $\mathbf{U}(n) = [\mathbf{U}_n \mathbf{U}_{n-1} \dots \mathbf{U}_{n-L+1}]^H$ and $\mathbf{g}(n) = [\mathbf{g}_n \mathbf{g}_{n-1} \dots \mathbf{g}_{n-L+1}]^H$. To this end, We have the following definitions:

$$\bar{\mathbf{U}}(n) = \begin{bmatrix} \mathbf{U}(n) \\ \mathbf{U}_{n-L}^H \end{bmatrix} = \begin{bmatrix} \mathbf{U}_n^H \\ \mathbf{U}(n-1) \end{bmatrix}, \quad (19)$$

and

$$\bar{\mathbf{g}}(n) = \begin{bmatrix} \mathbf{g}(n) \\ \mathbf{g}_{n-L}^H \end{bmatrix} = \begin{bmatrix} \mathbf{g}_n \\ \mathbf{g}(n-1) \end{bmatrix}. \quad (20)$$

The SWHH-RLS requires a two-step procedure for solving LS problem: an weight-update step and a down-date step. To this end, we can write for the weight-update step $\mathbf{h}(n-1) \rightarrow \bar{\mathbf{h}}(n) \rightarrow \mathbf{h}(n)$, with $\bar{\mathbf{h}}(n)$ being the solution of the LS problem obtained by replacing (19) and (20) in

(18), respectively for $\mathbf{U}(n)$ and $\mathbf{g}(n)$. For down-date part, we write [4], [35]

$$\mathbf{F}(n) = \bar{\mathbf{F}}(n) - \mathbf{U}_{n-L} \mathbf{U}_{n-L}^H. \quad (21)$$

Using Cholesky factors, equation (21) reads

$$\mathbf{T}^H(n) \mathbf{T}(n) = \bar{\mathbf{T}}^H(n) \bar{\mathbf{T}}(n) - \mathbf{U}_{n-L} \mathbf{U}_{n-L}^H. \quad (22)$$

The hyper normal matrix $\mathbf{H}(n)$ reads

$$\mathbf{H}(n) = \begin{bmatrix} \mathbf{U}_{n-L}^H \\ \bar{\mathbf{T}}(n) \end{bmatrix} = \begin{bmatrix} \mathbf{O}_{Q \times (N+1)} \\ \mathbf{T}(n) \end{bmatrix} \quad (23)$$

which is used to calculate $\mathbf{T}^{-1}(n)$ from $\bar{\mathbf{T}}^{-1}(n)$ using inverse Cholesky factor as [4], [35]

$$\mathbf{H}(n) = \begin{bmatrix} \mathbf{O}_{Q \times (N+1)} \\ \bar{\mathbf{T}}^{-T}(n) \end{bmatrix} = \begin{bmatrix} \mathbf{V}^H(n) \\ \mathbf{T}^{-T}(n) \end{bmatrix}, \quad (24)$$

where $\mathbf{V}(n)$ has dimensions $(N+1) \times Q$. Let us define the vector $\boldsymbol{\psi}(n) = -\bar{\mathbf{T}}^{-T}(n) \mathbf{U}_{n-L}$, then a hyper normal matrix $\mathbf{H}(n)$ is obtained in the form

$$\mathbf{H}(n) \begin{bmatrix} \mathbf{I}_Q \\ \boldsymbol{\psi}(n) \end{bmatrix} = \begin{bmatrix} \bar{\Delta}(n) \\ \mathbf{O}_{(N+1) \times Q} \end{bmatrix}, \quad (25)$$

with $\bar{\Delta}(n)$ is a square matrix and we defined $\mathbf{T}(n)$, $\boldsymbol{\psi}(n)$ and $\Delta(n)$ as in (19). Finally, the weight update is calculated recursively according to [4], [35]

$$\mathbf{h}(n) = \bar{\mathbf{h}}(n) + \mathbf{V}(n) \bar{\Delta}^{-T}(n) (\mathbf{g}_{n-L} - \mathbf{U}_{n-L}^H \bar{\mathbf{h}}(n)). \quad (26)$$

The complete steps of SWHH-RLS algorithm is summarized in Algorithm 4. Since the algorithm applies a window of size L on the input data and also the fact that the two-step procedures in Algorithm 4 are executed for $n > L$, it is therefore required to run the weight-update initialization L times and afterward the algorithm will transit to the two-step method discussed above.

4. NUMERICAL RESULTS

In this section, we present simulation results to assess the validity of the suggested Ball's based OFDM receiver, as shown in Fig. 3, using the four algorithms discussed in Sec. 3-A through Sec. 3-D. To this end, we consider time varying multipath Rayleigh fading channel with four paths specified with gains $G = [0 - 3 - 7 - 9]$ dB and delays $D = [0; 0.75; 1.66; 2.94]$ μs for LOS and the three NLOS respectively [37]. The FFT size is 64 with CP = 16 samples. The carrier frequency is $f_c = 800$ MHz and the sampling rate is $f_s = 6.78$ MHz at channel bandwidth BW = 20 MHz. The comb pilot is based on Superimposed Training Sequence (STS) technique used in [9]. We select the length of RLS filter as 80 and also Doppler shift as $f_d = 60$ Hz.

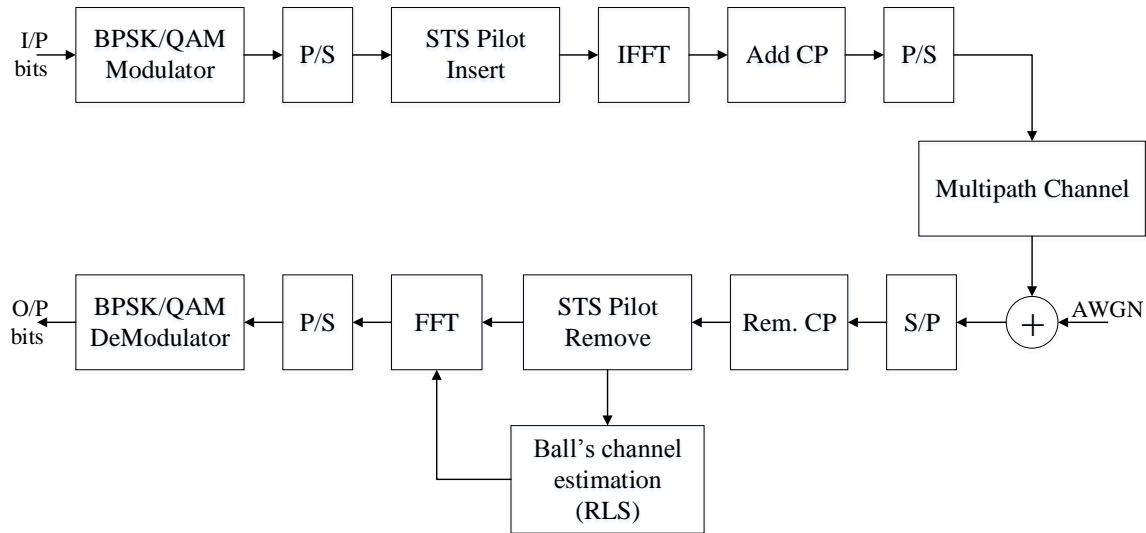


Figure 3. OFDM system using the proposed channel estimation scheme with CP and STS pilot. The blocks labeled as P/S and S/P denote parallel to serial and serial to parallel conversion, respectively.

Algorithm 4: SWHH-RLS algorithm

for all $n > L$ do

Step 1: Weight-update
 Computing: $\psi(n) = -\mathbf{T}^{-H}(n-1)\mathbf{U}_n$
 Computing $\Theta(n)$: $\Theta(n) \begin{bmatrix} \mathbf{I}_Q \\ \psi(n) \end{bmatrix} = \begin{bmatrix} \bar{\Delta}(n) \\ \mathbf{O}_{(N+1) \times Q} \end{bmatrix}$
 Updating $\mathbf{T}^{-1}(n-1)$: $\Theta(n) \begin{bmatrix} \mathbf{O}_{Q \times (N+1)} \\ \mathbf{T}^{-H}(n-1) \end{bmatrix} = \begin{bmatrix} \mathbf{E}^H(n) \\ \mathbf{T}^{-T}(n) \end{bmatrix}$
 Computing:
 $\hat{\mathbf{h}}(n) = \mathbf{h}(n-1) - \mathbf{E}(n)\bar{\Delta}^{-H}(n)(\mathbf{g}_k^* - \mathbf{U}_n^H \mathbf{h}(n-1))$
 Step 2: Down-date
 Computing $\bar{\psi}(n)$: $\bar{\psi}(n) = -\mathbf{T}^{-H}(n)\mathbf{U}_{n-L}$
 Computing $\mathbf{H}(n)$ using (24)
 Down-dating $\bar{\mathbf{T}}^{-1}(n)$:
 $\mathbf{H}(n) \begin{bmatrix} \mathbf{O}_{Q \times (N+1)} \\ \bar{\mathbf{T}}^{-H}(n) \end{bmatrix} = \begin{bmatrix} \mathbf{V}^H(n)\mathbf{T}^{-H}(n) \end{bmatrix}$
 Updating:
 $\mathbf{h}(n) = \hat{\mathbf{h}}(n) - \mathbf{V}(n)\bar{\Delta}^H(n)(\mathbf{g}_{n-L}^* - \mathbf{U}_{n-L}^H \hat{\mathbf{h}}(n))$

end

attributed to the fact that QRD-RLS and HH-RLS eliminate more errors compared to RLS due to the numerical stability and the reliable computation of the recursive least square problem.

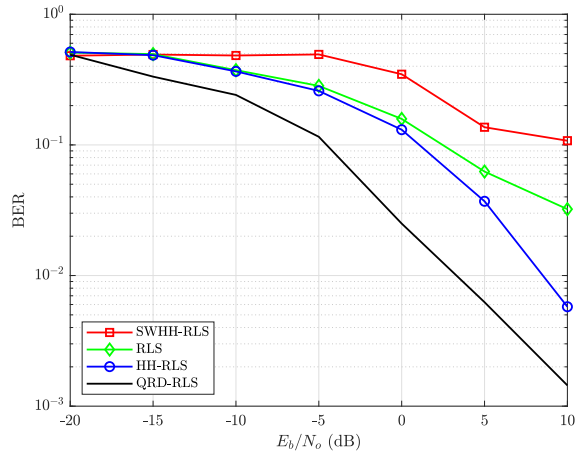


Figure 4. BER versus SNR for BPSK modulation.

Unless otherwise stated, we set the all initial coefficients (including $\mathbf{h}(0) = \mathbf{0}$) to zeros.

The Bit Error Rate (BER) versus the signal-to-noise ratio, in terms of E_b/N_0 , is plotted in Fig. 4 for BPSK modulation scheme. It is seen that QRD-RLS and HH-RLS algorithms provide better performance compared to traditional RLS. For instance, QRD-RLS provides performance gains of 15 dB and 8 dB compared to SWHH-RLS and RLS, respectively, at BER = 0.1. This improvement can be

Fig. 5 illustrates the Mean Square Error (MSE) versus the number of iterations required for the same algorithms outlined in Fig. 4. We first observe that the QRD-RLS algorithm, which provided the best BER performance in Fig. 4, have slower convergence rate that requires about 2000 iterations to reach MSE less than 0.2, compared to the conventional RLS algorithm. This is a direct result from the fact that this algorithm is stable and yield better performance at the cost of having more computational

complexity. The figure also confirms that RLS and HH-RLS reach typical convergence with less than 500 iterations.

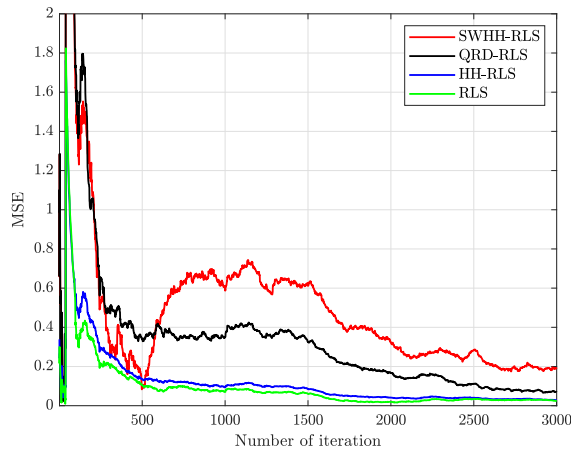


Figure 5. MSE versus iteration number for BPSK modulation.

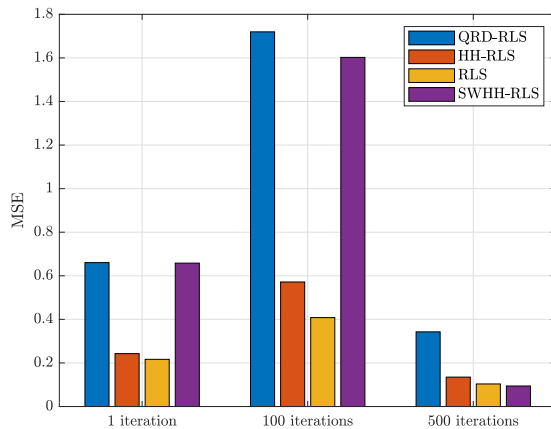


Figure 6. Numerical comparison of MSE of the four algorithms considered in Fig. 5 using Bar graph. The figure shows MSE after 1, 100 and 500 iterations with BPSK modulation.

To provide more insight about the convergence behavior of the proposed scheme, we present in Fig. 6 a numerical comparison of the MSE, which is computed numerically from (4), for the considered algorithms after 1, 100 and 500 iterations. Inline with the results from Fig. 5, this figure confirms the observation that QRD-RLS yields the worst MSE performance compared to the other algorithm which reaches moderate MSE (≤ 0.4) after 500 iterations. In addition, RLS and HH-RLS maintain the least MSE performance during iterations. The latter case is attributed to the fact that the rapid convergence comes at the cost of having higher BER performance as seen in Fig. 4.

Finally, in order to shed light on the effect of the

modulation type on the suggested scheme, Fig. 7 adopt a 16-QAM modulation scheme for the same set-up studied in Fig. 4. Numerically, it is noted that the performance of QRD-RLS outperforms HH-RLS and RLS by 2 dB and 10 dB, respectively, at BER = 0.2. This improvement is attributed to the same reasons discussed in the comments on Fig. 4.

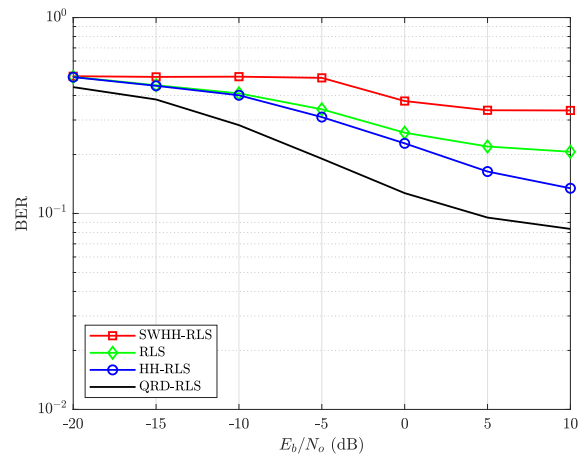


Figure 7. BER versus SNR for 16-QAM modulation.

5. CONCLUDING REMARKS

This paper considers the evaluation of a novel OFDM receiver, that incorporate Ball's adaptive channel estimation scheme, over fading channels. The performance evaluation, as measured in terms of BER and MSE learning curve, illustrates that RLS and HH-RLS algorithms show faster convergence rate and low miss-adjustment at steady states compared to other RLS-type algorithms, while QRD-RLS algorithm achieves the best BER performance. As a final remark, the HH-RLS strikes a good balance in providing moderate BER performance gain while maintaining acceptable convergence properties. Among the future directions for this study are the incorporation of the proposed scheme in massive MIMO OFDM systems.

REFERENCES

- [1] A. Goldsmith, *Wireless Communications*. USA: Cambridge University Press, 2005.
- [2] Proakis, *Digital Communications 5th Edition*. McGraw Hill, 2007.
- [3] S. Haykin, *Adaptive Filter Theory (3rd Ed.)*. USA: Prentice-Hall, Inc., 1996.
- [4] B. Widrow and S. D. Stearns, *Adaptive Signal Processing (3rd Ed.)*. Englewood Cliffs, N.J., USA: Prentice-Hall, Inc., 1985.
- [5] A. N. Al-Shuwaili, A. Bagheri, and O. Simeone, "Joint up-link/downlink and offloading optimization for mobile cloud com-



- puting with limited backhaul," in *2016 Annual Conference on Information Science and Systems (CISS)*, pp. 424–429, March 2016.
- [6] A. Al-Shuwaili and A. Lawey, "Latency reduction for mobile edge computing in hetnets by uplink and downlink decoupled access," *IEEE Wireless Communications Letters*, vol. 10, no. 10, pp. 2205–2209, 2021.
- [7] T. Hwang, C. Yang, G. Wu, S. Li, and G. Ye Li, "Ofdm and its wireless applications: A survey," *IEEE Transactions on Vehicular Technology*, vol. 58, no. 4, pp. 1673–1694, 2009.
- [8] W. Ahmed and M. J. Al-Kindi, "Adaptive direct channel estimation in OFDM system using Superimposed Training Sequence (STS) technique," *International Journal of Scientific and Engineering Research (IJSER)*, vol. 9, no. 9, pp. 364–373, June 2018.
- [9] J. K. Tugnait and Xiaohong Meng, "On superimposed training for channel estimation: performance analysis, training power allocation, and frame synchronization," *IEEE Transactions on Signal Processing*, vol. 54, no. 2, pp. 752–765, Feb 2006.
- [10] Y. Liu, Z. Tan, H. Hu, L. J. Cimini, and G. Y. Li, "Channel estimation for ofdm," *IEEE Communications Surveys Tutorials*, vol. 16, no. 4, pp. 1891–1908, 2014.
- [11] S. Coleri, M. Ergen, A. Puri, and A. Bahai, "Channel estimation techniques based on pilot arrangement in ofdm systems," *IEEE Transactions on Broadcasting*, vol. 48, no. 3, pp. 223–229, 2002.
- [12] M.-H. Hsieh and C.-H. Wei, "Channel estimation for ofdm systems based on comb-type pilot arrangement in frequency selective fading channels," *IEEE Transactions on Consumer Electronics*, vol. 44, no. 1, pp. 217–225, 1998.
- [13] O. Simeone, Y. Bar-Ness, and U. Spagnolini, "Pilot-based channel estimation for ofdm systems by tracking the delay-subspace," *IEEE Transactions on Wireless Communications*, vol. 3, no. 1, pp. 315–325, 2004.
- [14] M. Soltani, V. Pourahmadi, A. Mirzaei, and H. Sheikhzadeh, "Deep learning-based channel estimation," *IEEE Communications Letters*, vol. 23, no. 4, pp. 652–655, 2019.
- [15] M. Morelli and U. Mengali, "A comparison of pilot-aided channel estimation methods for ofdm systems," *IEEE Transactions on Signal Processing*, vol. 49, no. 12, pp. 3065–3073, 2001.
- [16] B. Yang, Z. Cao, and K. Letaief, "Analysis of low-complexity windowed dft-based mmse channel estimator for ofdm systems," *IEEE Transactions on Communications*, vol. 49, no. 11, pp. 1977–1987, 2001.
- [17] H. Ye, G. Y. Li, and B.-H. Juang, "Power of deep learning for channel estimation and signal detection in ofdm systems," *IEEE Wireless Communications Letters*, vol. 7, no. 1, pp. 114–117, 2018.
- [18] L. Li, H. Chen, H.-H. Chang, and L. Liu, "Deep residual learning meets ofdm channel estimation," *IEEE Wireless Communications Letters*, vol. 9, no. 5, pp. 615–618, 2020.
- [19] J. Liu, K. Mei, X. Zhang, D. Ma, and J. Wei, "Online extreme learning machine-based channel estimation and equalization for ofdm systems," *IEEE Communications Letters*, vol. 23, no. 7, pp. 1276–1279, 2019.
- [20] R. Jiang, X. Wang, S. Cao, J. Zhao, and X. Li, "Deep neural networks for channel estimation in underwater acoustic ofdm systems," *IEEE Access*, vol. 7, pp. 23 579–23 594, 2019.
- [21] Y.-S. Jeon, N. Lee, and H. V. Poor, "Robust data detection for mimo systems with one-bit adcs: A reinforcement learning approach," *IEEE Transactions on Wireless Communications*, vol. 19, no. 3, pp. 1663–1676, 2020.
- [22] G. Stuber, J. Barry, S. McLaughlin, Y. Li, M. Ingram, and T. Pratt, "Broadband mimo-ofdm wireless communications," *Proceedings of the IEEE*, vol. 92, no. 2, pp. 271–294, 2004.
- [23] Y. Liao, Y. Hua, and Y. Cai, "Deep learning based channel estimation algorithm for fast time-varying mimo-ofdm systems," *IEEE Communications Letters*, vol. 24, no. 3, pp. 572–576, 2020.
- [24] H. Minn and N. Al-Dhahir, "Optimal training signals for mimo ofdm channel estimation," *IEEE Transactions on Wireless Communications*, vol. 5, no. 5, pp. 1158–1168, 2006.
- [25] C. Shin, R. W. Heath, and E. J. Powers, "Blind channel estimation for mimo-ofdm systems," *IEEE Transactions on Vehicular Technology*, vol. 56, no. 2, pp. 670–685, 2007.
- [26] F. Wan, W.-P. Zhu, and M. N. S. Swamy, "A semiblind channel estimation approach for mimo-ofdm systems," *IEEE Transactions on Signal Processing*, vol. 56, no. 7, pp. 2821–2834, 2008.
- [27] —, "Semiblind sparse channel estimation for mimo-ofdm systems," *IEEE Transactions on Vehicular Technology*, vol. 60, no. 6, pp. 2569–2582, 2011.
- [28] H. Minn and V. Bhargava, "An investigation into time-domain approach for ofdm channel estimation," *IEEE Transactions on Broadcasting*, vol. 46, no. 4, pp. 240–248, 2000.
- [29] C.-S. Yeh and Y. Lin, "Channel estimation using pilot tones in ofdm systems," *IEEE Transactions on Broadcasting*, vol. 45, no. 4, pp. 400–409, 1999.
- [30] H. Abbood, H. Khazal, and T. Jamel, "Time domain pilot-based channel estimation (tdpce) using kalman filtering for ofdm system," *IOP Conference Series: Materials Science and Engineering*, vol. 1090, p. 012064, 03 2021.
- [31] C. Suh, C.-S. Hwang, and H. Choi, "Comparative study of time-domain and frequency-domain channel estimation in mimo-ofdm systems," in *14th IEEE Proceedings on Personal, Indoor and Mobile Radio Communications, 2003. PIMRC 2003.*, vol. 2, 2003, pp. 1095–1099 vol.2.
- [32] Z. Cheng and D. Dahlhaus, "Time versus frequency domain channel estimation for ofdm systems with antenna arrays," in *6th International Conference on Signal Processing, 2002.*, vol. 2, 2002, pp. 1340–1343 vol.2.
- [33] B. Zheng and R. Zhang, "Intelligent reflecting surface-enhanced

ofdm: Channel estimation and reflection optimization," *IEEE Wireless Communications Letters*, vol. 9, no. 4, pp. 518–522, 2020.

- [34] B. Zheng, C. You, and R. Zhang, "Fast channel estimation for irs-assisted ofdm," *IEEE Wireless Communications Letters*, vol. 10, no. 3, pp. 580–584, 2021.
- [35] J. Apolinário, *QRD-RLS Adaptive Filtering*. Boston, MA: Springer., 2009.
- [36] S. Khanom and M. R. Islam, "Performance analysis of QR-decomposition RLS and householder sliding window RLS for noise elimination of EEG," in *2017 IEEE Region 10 Humanitarian Technology Conference (R10-HTC)*, Dec 2017, pp. 594–597.
- [37] A. Al-Shuwaili and T. M. Jamel, "5G channel characterization at millimeter-wave for baghdad city: An NYUSIM-based approach," in *2021 18th International Multi-Conference on Systems, Signals Devices (SSD)*, 2021, pp. 468–473.



Ali Al-Shuwaili Ali Al-Shuwaili gained a Ph.D. degree in electrical engineering from New Jersey Institute of Technology (NJIT), Newark 07012, NJ, USA. Before that, he received the M.Sc. and B.Sc. degrees in communication engineering from Electrical and Electronic Engineering (EEE) department at University of Technology, Baghdad, Iraq, in 2005 and 2008, respectively. He

worked in telecommunication industry with ZTE and mSolutions companies and currently he holds an active research position and teaching position at UOITC. His research interests are in wireless communication, optimization and machine learning.



Mustafa Dh. Hassib Mustafa Dh. Hassib was born in Baghdad, Iraq. He received his B.Eng. degree in Electronics and Communications engineering from the University of Technology Iraq, in 1991 and his M.Sc. degree in Communications engineering from the Military engineering college at Baghdad, Iraq in 2004 and the Ph.D. degree in mobile wireless communications from the National

University of Malaysia (UKM), in 2015. He has held various positions in the Department of communications at the University of Technology Iraq. His research interests take account of mobile wireless communication, Optical communication and coding theory.



Thamer M. Jamel Thamer M. Jamel graduated from the University of Technology with a Bachelor's degree in electronics engineering. He received a Master's and a Doctoral degree in communication engineering in 1997. His scientific degree is Professor and currently, he is one of the staff of the communication engineering department at University of Technology, Baghdad, Iraq.

His Research Interests are Adaptive Digital Signal Processing (Algorithms and Applications) for modern and future Communications system.